[Frontiers in Bioscience E3, 834-842, June 1, 2011]

AIG1 is a novel Pirh2-interacting protein that activates the NFAT signaling pathway

Gang Wu[1, 2], Meiqian Sun[3], Wei Zhang[1], Keke Huo[1]

[1] State Key Laboratory of Genetic Engineering, Institute of Genetics, School of Life Sciences, Fudan University, 220 Handan Rd., Shanghai 200433, PR China, [2] Chinese Academy of Sciences and Max Planck Society (CAS-MPG) Partner Institute for Computational Biology, Shanghai Institutes for Biological Sciences, Chinese Academy of Sciences, 320 Yue Yang Rd., Shanghai 200031, PR China, [3] United Gene Bio-Pharma Inc. , 100 Handan Rd., Shanghai 200437, PR China

TABLE OF CONTENTS

1. ABSTRACT

Pirh2 is an E3 ligase that negatively regulates p53 through both direct physical interaction and ubiquitin-mediated proteolysis. Here, we identified a novel Pirh2-interacting protein, AIG1, by yeast two-hybrid screening and confirmed its interaction with p53 both *in vitro* and *in vivo*. Quantitative real-time reverse transcription-PCR analysis showed that *AIG1* expression levels were reduced in 50 out of 79 (63%) human hepatocellular carcinomas (HCCs) when compared to matched, non-cancerous liver tissue; levels were significantly different between HCCs with or without lymph node metastasis. Kaplan-Meier analysis indicated that the survival time of HCC patients down-regulated for *AIG1* is much shorter than it is for patients up-regulated for *AIG1* expression (p = 0.0313 as determined by the Log-rank test). Finally, AIG1 activated the nuclear factor of activated T cells (NFAT) signaling pathway in a dose-dependent manner when over-expressed in HEK293T cells. Our results suggest AIG1 could serve as a new biomarker for the diagnosis and prognostic evaluation of HCCs.

2. INTRODUCTION

Hepatocellular carcinoma (HCC) is one of the most frequent malignancies worldwide with an estimated annual incidence of 1 million cases (1). It is the fifth most common cancer and the third-leading cause of cancer-related deaths (2-4). Although the highest incidence rates of HCCs are found in Africa and Asia, there has been a steady, overall increase across most Western nations over the last two decades (5, 6). HCCs primarily occur in chronically diseased livers as a result of hepatitis virus infections, aflatoxin exposure or alcohol consumption. However, the pathogenic mechanisms responsible for inducing HCC formation are still undefined.

The development of HCC is a multistep process associated with changes in host gene expression, some of which correlate with the appearance and progression of tumor formation (7). To date, many important genes responsible for the genesis of various cancers have been discovered, their mutations precisely identified and the pathways through which they act characterized (8).

Notably, the number of studies on the altered gene expression within HCCs has recently increased, and a number of genes that are either up- or down-regulated, or lost entirely in HCCs have been reported (9-13). However, the identification of these alternatively regulated genes has yet to fully explain the mechanisms of HCC formation. Additionally, the complete list of genes involved in HCC development is still likely to be incomplete.

The p53-induced RING-H2 protein (Pirh2) was a newly identified RING-H2-type E3 ligase, also known as androgen receptor N-terminal interacting protein (ARNIP) (14), which can negatively regulate p53 through both direct physical interaction and ubiquitin-mediated proteolysis independent of Mdm2 (15). Our previous studies confirmed that Pirh2 can also interact with SCYL1-BP1 and degrade SCYL1-BP1 through the ubiquitin-proteasome pathway (16, 17). We recently reported that the expression level of Pirh2 was reduced at both the transcriptional and the translational level in HCCs relative to matched, non-cancerous liver tissues (18). The altered expression profile of Pirh2 was also documented in many other kinds of human carcinomas including prostatic carcinoma, lung cancer, and head and neck cancer (19-21), suggesting that Pirh2 could potentially be used as a general prognostic biomarker in addition to serving as a novel target for anti-cancer drug therapies.

Here, we report the identification of a novel Pirh2-interacting protein, androgen-induced 1 (AIG1), which was initially cloned from human dermal papilla cells (22) and is evolutionally conserved from drosophila through to humans. We demonstrate here, for the first time, the down-regulation of AIG1 in HCCs and the activation of the NFAT signaling pathway by AIG1. The correlation between AIG1 expression and HCC clinicopathologic characteristics, as well as the survival of patients with HCC after hepatic resection, were analyzed to explore the prognostic value of AIG1. These results not only shed light on the functional relationship between AIG1 and Pirh2 but should also stimulate further investigation into the significance of the interaction between Pirh2 and AIG1.

3. MATERIALS AND METHODS

3.1. Yeast two-hybrid screening

A human fetal liver MATCHMAKER cDNA library (Clontech) was used for yeast two-hybrid screening. The full-length *Pirh2* open reading frame was cloned into the pGBKT7 vector to generate the bait plasmid. The pGBKT7- Pirh2 and the library plasmids were sequentially transformed into yeast host strain AH109. A total of 3.67×10^6 transformants were plated onto the SD/-Ade/-His/-Leu/-Trp plates, and incubated for 3-4 days at 30 °C. Plasmids were rescued from the positive clones and used for mating tests to confirm that these interactions were specific. Plasmids from confirmed interactors were then isolated, sequenced and identified using the BLAST algorithm from the NCBI website (www.ncbi.nlm.nih.gov/BLAST).

3.2. GST pull-down assay

The full coding sequences of *AIG1* and *Pirh2* were each cloned into the pGEX-5X-1 (Amersham Pharmacia Biotech) and pET-32a (+) (Novagen) vectors, respectively. The GST-AIG1 fusion protein was expressed in *E. coli* strain BL21 and induced with 0.1 mM IPTG at 28 °C for 1 h. The His-Pirh2 fusion protein was expressed in *E. coli* strain BL21 (DE3), induced with 0.1 mM IPTG at 22 °C for 6 h and then purified by Ni-NTA Agarose (QIAGEN). The remainder of the GST pull-down assay was performed as previously described (23).

3.3. Cell culture and co-immunoprecipitation assay

HEK293T cells were maintained in Dulbecco's modified Eagle's medium (DMEM) supplemented with 10% bovine calf serum (GIBCO) and grown on 60-mm dishes at a concentration of 6×10^5 cells/dish one day prior to transfection. The complete coding sequences of *Pirh2* and *AIG1* were inserted in-frame into the vectors pCMV-Myc and pCMV-HA (Clontech), respectively, which were then transfected into cells using Lipofectamine 2000 (Invitrogen). After 48 h, cells were washed twice with ice-cold PBS and lysed with 400 ul of lysis buffer (Roche). Cell lysates were clarified by centrifugation at 15,000 rpm for 15 min at 4 °C and precleared with protein A/G agarose (Santa Cruz, CA) for 1 h. The supernatants were incubated with 1-2 μg of relevant antibody bound to protein A/G agarose beads at 4 °C overnight. After washing three times with lysis buffer, the precipitates were electrophoretically separated on 12% SDS-PAGE gels, which were then used for western blotting.

3.4. *In vivo* ubiquitination assay

HEK293T cells were transfected with pCMV-HA-AIG1 and pcDNA3.1-FLAG-ubiquitin in combination with either empty pCMV-Myc or pCMV-Myc-Pirh2. After 18 h, cells were treated with 10 μM MG-132 (Sigma-Aldrich) for an additional 6 h, lysed with a modified RIPA buffer (2 mM Tris-HCl [pH 7.5], 5 mM EDTA, 150 mM NaCl, 1% NP-40, 1% deoxycholate, 1% SDS and 1 mM PMSF) and then analyzed by IP/immunoblotting. For immunoprecipitation, the lysates were sonicated for 6 seconds and clarified by centrifugation at 4 °C for 15 min to remove cellular debris. Lysates (1 mg) were then incubated with an anti-FLAG antibody (Sigma-Aldrich). The immunoprecipitates were collected with protein A/G agarose beads, washed with RIPA buffer, separated on 10% SDS-PAGE gels and analyzed by western blotting.

3.5. Subcellular localization analysis

Hela cells were cultured in DMEM, supplemented with 10% fetal bovine serum (Life Technologies) at 37 °C with 5% CO2. The complete *AIG1* ORF was cloned in-frame with the fluorescence tag in the pDsRed1-N1 plasmid (Clontech), which fused RFP to the C-terminus of AIG1. Hela cells grown on cover slips were transiently transfected with the pDsRed1-N1-AIG1 plasmid. *Pirh2* was cloned into the pEGFP-C1 plasmid (Clontech) to generate the expression construct pEGFP-C1-Pirh2, which fused GFP to the N-terminus of Pirh2. HEK293T cells were used for the subcellular co-localization experiments with pEGFP-C1-Pirh2 and pDsRed1-N1-AIG1. Cells were fixed 48 h after transfection with 4% formaldehyde and stained with 1 ug/ml 4',6'-diamidino-2-phenylindole (DAPI) for

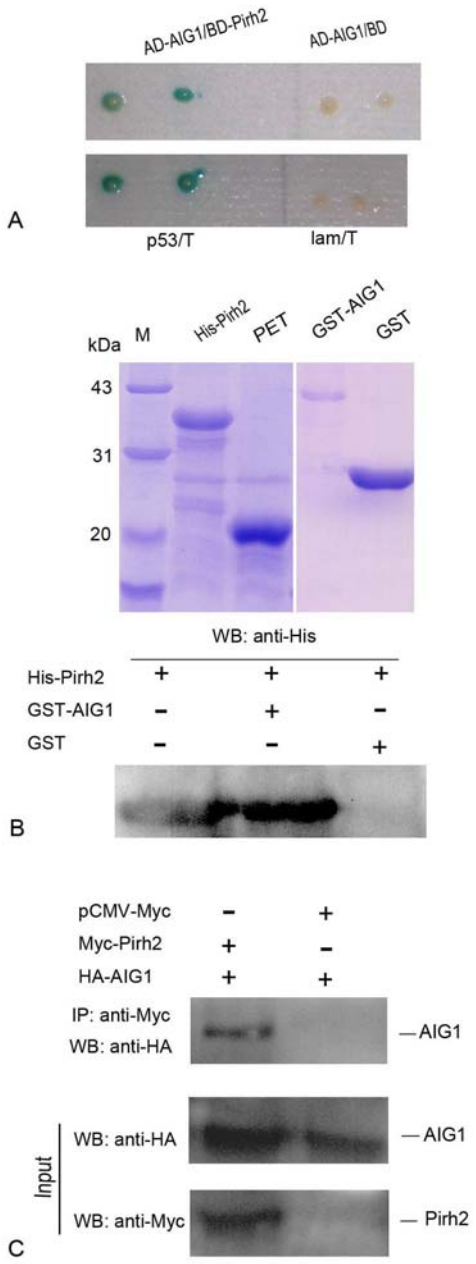

Figure 1. Pirh2 interacts with AIG1 *in vitro* and *in vivo*. (A) Yeast two-hybrid interaction between Pirh2 and AIG1. Beta-galactosidase assay was used to detect interaction. AD-AIG1/BD-Pirh2 (pGADT7-AIG1/pGBKT7-Pirh2) showed positive interaction, but this was absent in AD-AIG1/BD (pGADT7-AIG1/pGBKT7). p53/T and lam/T are the positive and negative control, respectively. (B) His-Pirh2, PET, GST-AIG1 and GST were expressed and purified. His-Pirh2 binds to GST-AIG1 but not to GST alone. His-Pirh2 expressed in *E. coli* BL21 (DE3) was used as the control. (C) Pirh2 interacts with AIG1 *in vivo*. Myc-Pirh2 and HA-AIG1 were co-transfected into HEK293T cells. Myc tagged vector and HA-AIG1 were co-transfected as the control. Lysate was immunoprecipitated with anti-Myc antibody and analyzed by immunoblotting with anti-HA antibody.

nuclei visualization. Analysis of fluorescent images was performed with the Olympus IX71 laser microscope.

3.6. Quantitative real-time reverse transcription-PCR

Total RNA derived from normal and tumor tissues collected from HCC patients undergoing surgery at Shanghai Zhong Shan Hospital, were extracted by TRIzol (GibcoBRL) and then treated with amplification-grade DNase I (Invitrogen) before cDNA synthesis. Reverse transcription was carried out with a Reverse Transcriptase Kit (TaKaRa) and qPCR was performed in triplicate using the SYBR Green Mastermix on the ABI Prism 7900 Sequence Detection System (Applied Biosystems). *GAPDH* was used as an endogenous control, and data were analyzed using the comparative threshold cycle ($2^{-\Delta\Delta CT}$) method (24). qPCR conditions used for amplification were 95 °C for 15 min, followed by 40 cycles of 95 °C for 15 s and 60 °C for 1 min. Final PCR products were analyzed by melt curve analysis: 95 °C for 15 s, 60 °C for 15 s and 95 °C for 15 s. PCR primer sequences used were as follows: *AIG1*, 5'-GGGACTGGATGTTAGCTGTG-3' (sense), 5'-GGATACTGATGGTGCGATGT-3' (antisense); *GAPDH*, 5'-GCACCGTCAAGGCTGAGAAC-3' (sense), 5'-ATGGTGGTGAAGACGCCAGT-3' (antisense).

3.7. Pathway profiling assay

HEK293T cells were seeded the day prior to transfection at a density of $1x10^5$ cells per well in 24-well plates. Cells were transfected with 100 ng of reporter plasmids pAP1-Luc, pSRE-Luc, pGRE-Luc, pHSE-Luc, pNF-kappaB-Luc, pAP1(PMA)-Luc, pp53-Luc, pP21-Luc, pMyc-Luc, pNFAT-Luc, pE2F-Luc or pRb-Luc (Clontech) individually in addition to 300 ng of pCMV-HA-AIG1 or pCMV-HA. Cells were also transfected with 10 ng of pRL-SV40 (Promega), which encodes the *Renilla* luciferase gene and served as the internal control. After incubation for 6 h, transfection complexes were removed from the wells and cells were washed with media. Transfected reporters were then induced by maintaining cells under serum starvation conditions in DMEM containing only 0.4% FBS. After 12 h, the transfected cells were lysed, and luciferase reporter activities were determined with the Dual-Luciferase Reporter Assay System on the GloMax 96 Luminometer (Promega). Levels of reporter gene induction were calculated by normalizing firefly luciferase activities to total *Renilla* luciferase levels. Results are presented as means +/- standard deviation (SD) and summarize data from three independent experiments, each conducted in duplicate. These luciferase results were used to determine if it was necessary to assay AIG1 activation of the NFAT signaling pathway in a dose-dependent manner.

3.8. Statistical analysis

The relationship between *AIG1* expression levels, the clinicopathologic factors of HCC and the results of the luciferase reporter assays were assessed for statistical significance by the Student's *t*-test and the two-sample Kolmogorov-Smirnov test. Survival was estimated using the Kaplan–Meier method and the Log-rank test was used for comparison of survival curves. All analyses were performed using SPSS 12.0 software (Chicago, IL). Results were considered to be statistically significant if $p < 0.05$.

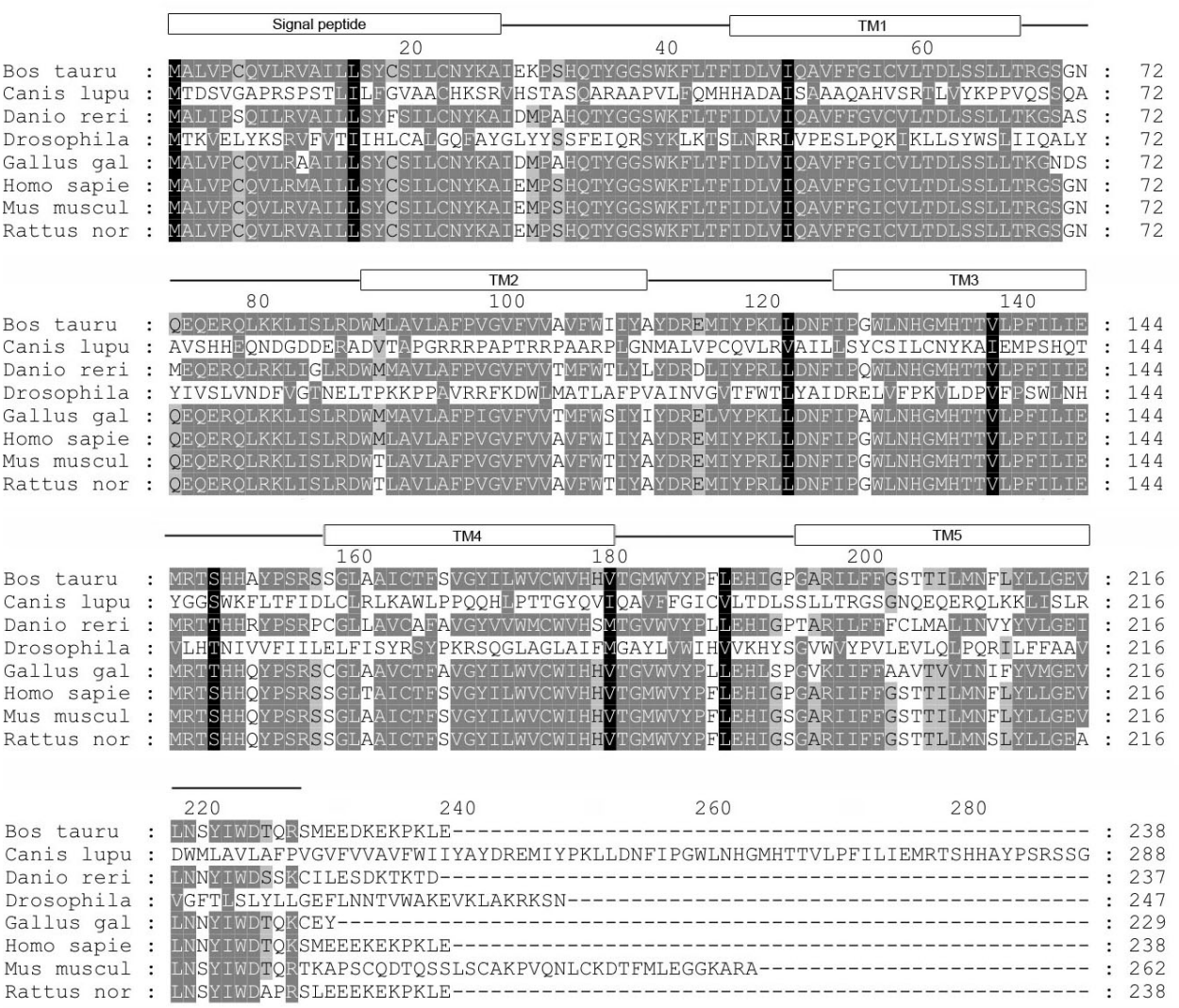

Figure 2. Multiple alignment of AIG1 with its homologs. Alignment of homo spaie AIG1 (NP_057192) with its seven homologs: Bos tauru (NP_001069794), Canis lupu (XP_854469), Danio reri (XP_690746), Drosophila (NP_722622), Gallus gal (XP_419710), Mus muscul (NP_079722) and Rattus nor (XP_214790) was carried out using GeneDoc program. Similar residues in at least three fourths of the sequences are shadowed (the residues conserved in all the sequences are indicated by a black background). Five transmembrane (TM) hydrophobic helices (open boxes) are linked by an extensive hydrophilic region (solid lines).

4. RESULTS

4.1. Pirh2 interacts with AIG1 *in vitro* and *in vivo*

To identify novel Pirh2-interacting proteins, a human fetal liver cDNA library was screened by yeast two-hybrid, which identified 13 positive clones from a total of 3.67×10^6 transformants. Sequence analysis showed that 4 of the 13 clones encode full-length *AIG1* (GenBank accession No. NM_016108). To confirm this result, pGBKT7-Pirh2 and pGADT7-AIG1 were transformed into yeast strains AH109 and Y187, respectively, and used for mating test analysis. As expected, strong activation of the reporter genes was observed, thus confirming the Pirh2-AIG1 interaction (Figure 1A). To validate the physical interaction between Pirh2 and AIG1 *in vitro*, a GST pull-down assay was performed. Glutathione-sepharose beads conjugated to bacterially expressed GST-AIG1, but not GST alone, were able to specifically pull-down His-tagged Pirh2 (Figure 1B). To further verify whether Pirh2 interacts with AIG1 *in vivo*, a co-immunoprecipitation assay was carried out in HEK293T cells transiently co-transfected with Myc-tagged Pirh2 and HA-tagged AIG1. Assay of immunoprecipitated Myc-Pirh2 samples also detected AIG1, thereby confirming the interaction between the two proteins (Figure 1C).

4.2. AIG1 is a conserved protein and can co-localize with Pirh2

BLAST analysis of AIG1 revealed that it is conserved in fruit flies, zebrafish, chickens and mammals.

Table 1. Summary of the relationship between *AIG1* expression levels and the clinicopathological features of 79 patients diagnosed with HCC

Clinical features	Variable	No. of cases	AIG1 expression (ΔCt)	*p*-value
Gender	Male	68	0.09 +/- 0.01	0.40
	Female	11	0.14 +/- 0.05	
Age (y)	< 50	34	0.08 +/- 0.01	0.84
	≥ 50	45	0.11 +/- 0.02	
Tumor size (cm)	< 5	47	0.09 +/- 0.01	0.72
	≥ 5	32	0.11 +/- 0.02	
Serum AFP (ng/ml)	≤ 100	31	0.10 +/- 0.01	0.64
	> 100	48	0.11 +/- 0.02	
Lymph node metastasis	+	43	0.10 +/- 0.01	0.03
	-	36	0.12 +/- 0.01	
Differentiation	I	17	0.13 +/- 0.04	0.73
	II	43	0.09 +/- 0.01	
	III	19	0.09 +/- 0.01	
Liver cirrhosis	+	20	0.08 +/- 0.01	0.44
	-	59	0.12 +/- 0.02	
Vascular invasion	+	10	0.10 +/- 0.01	0.94
	-	69	0.08 +/- 0.01	

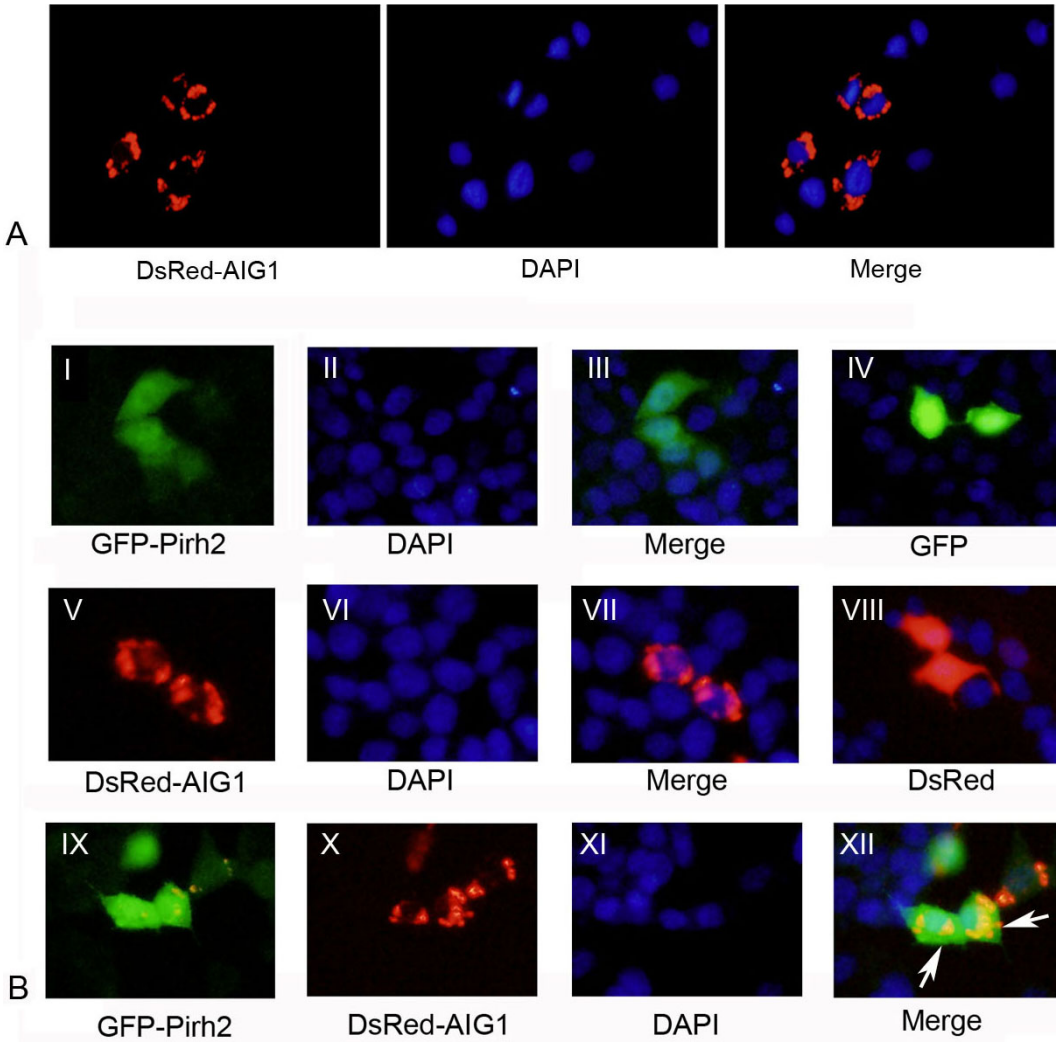

Figure 3. Subcellular localization analysis. (A) RFP-tagged AIG1 (DsRed-AIG1) distributes in the limited area immediately surrounding the nuclei in Hela cells. (B) HEK293T cells were transfected with pEGFP-C1-Pirh2 (GFP-Pirh2, I-III), pEGFP-C1 (GFP control, IV), DsRed1-AIG1 (V-VII), pDsRed1-N1 (DsRed control, VIII) or a combination of GFP-Pirh2 and DsRed1-AIG1 (IX-XII). Arrows indicate that Pirh2 co-localizes with AIG1. Nuclei were stained by DAPI.

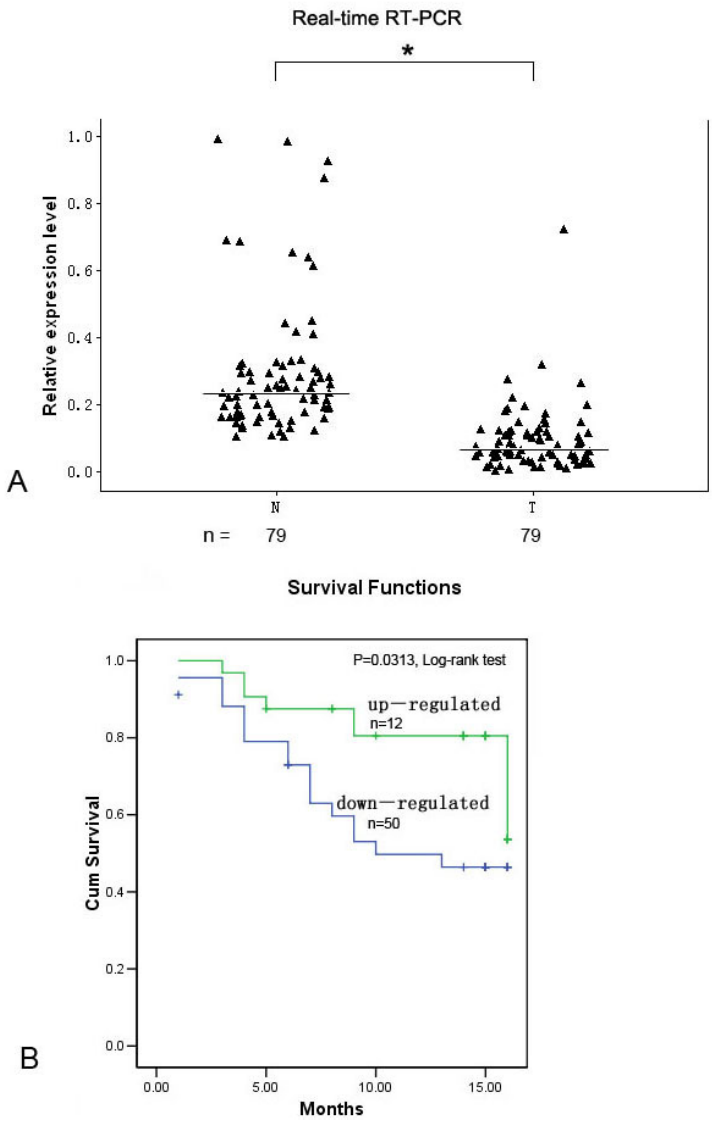

Figure 4. Significant down-regulation of AIG1 gene expression in HCC and Kaplan-Maier survival analysis. (A) Gene expression of AIG1 is determined by real time RT-PCR. Numbers of non-cancerous (N, ▲) and paired cancerous samples (T, ▲) used in the study are indicated. Bars represent median values. Asterisk denotes a significant difference at $p<0.0001$ when compared using Two-sample Kolmogorov-Smirnov test. (B) The Kaplan-Maier method was used to determine patient survival, and the Log-rank test was used to compare survival between subgroups. HCC patients were divided into two groups, the *AIG1* up-regulated group (green line) and the *AIG1* down-regulated group (blue line). The survival time of HCC patients down-regulated for *AIG1* is much shorter than it is for patients up-regulated for *AIG1* expression ($p = 0.0313$, Log-rank test). Cum. Survival means the survival probability. Survival time was constructed from the diagnosis date of HCC until the date of death or the date of the last follow-up.

SMART analysis (http://smart.embl-heidelberg.de/) revealed a predicted signal peptide in the N-terminus of AIG1 (1-26 aa) as well as a FAR-17a domain (36-223 aa), which contains five transmembrane segments (Figure 2). To determine if AIG1 could be a transmembrane protein, the subcellular localization of AIG1 was examined. As shown in Figure 3A, we found that in Hela cells AIG1 is primarily located proximal to the nuclei, suggesting that the protein is at least partially localized to nuclear membrane. Moreover, GFP-Pirh2 exhibits a diffuse nuclear and cytoplasmic localization, which is in agreement with previously published reports (19, 25, 26). RFP-tagged AIG1 and GFP-tagged Pirh2 were also found to co-localize in HEK293T cells (Figure 3B), further confirming the interaction between AIG1 and Pirh2.

4.3. Expression of AIG1 in HCCs compared to non-cancerous tissues

To test if *AIG1* expression is linked to liver cancer, we examined mRNA levels of *AIG1* by qRT-PCR

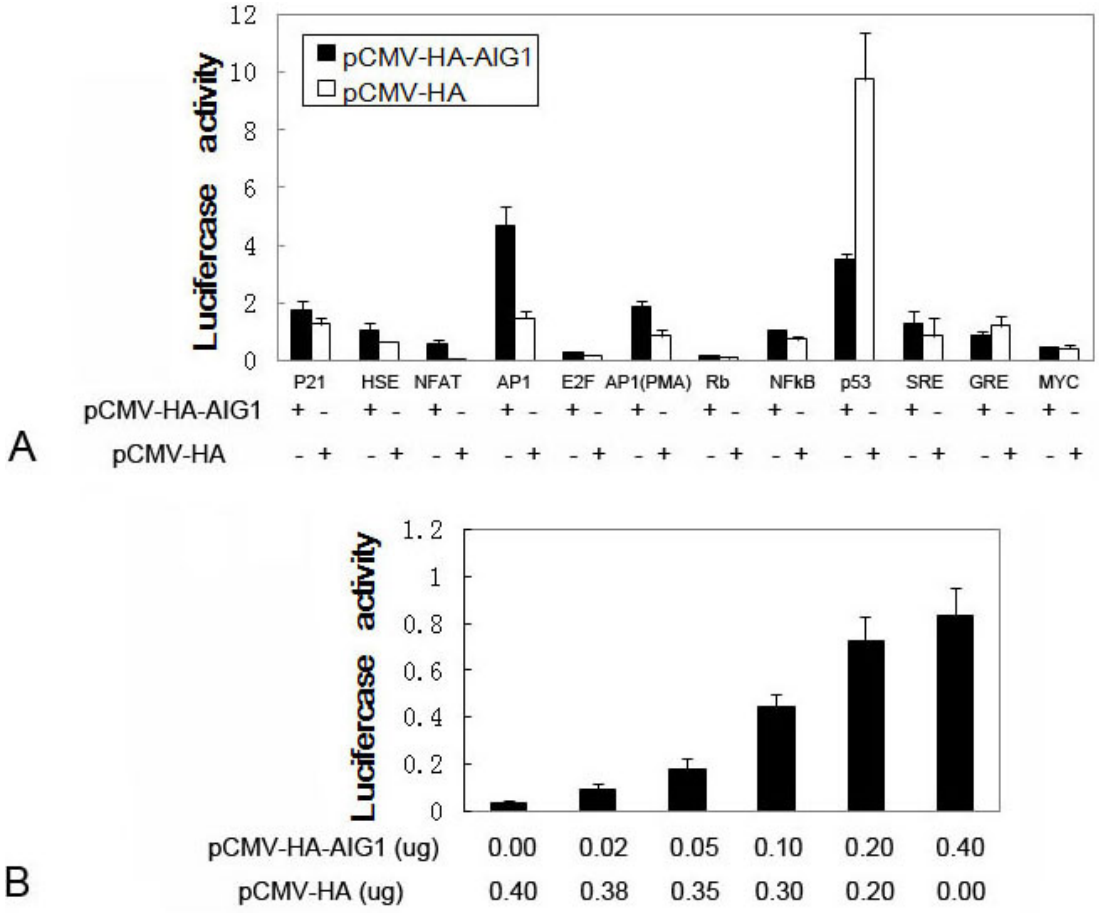

Figure 5. Transcriptional function analysis of AIG1. (A) The transcriptional activities of NFAT- and AP1-lucifercase activity were significantly increased about 1190% and 316%, respectively. Additionally, p53-luciferase activity was strongly decreased, by about 64.1%. (B) Dose-dependent activation of NFAT-luciferase by AIG1. The transfected amounts of pCMV-HA-AIG1 and pCMV-HA are shown in the figure.

analysis in 79 pairs of HCC and non-cancerous tissues. We found that *AIG1* levels were lower in 63% of HCC cases (50/79) than in normal liver tissues. After normalizing the expression level of *AIG1* in each sample with *GAPDH* mRNA levels, we found that *AIG1* was significantly down-regulated in HCCs (Figure 4A). We further investigated the correlation between *AIG1* levels and the clinical features of HCCs (Table 1) and found that statistically significant differences in the levels of *AIG1* were observed between HCCs with or without lymph node metastasis.

Based on the results of the *AIG1* qRT-PCR, 79 HCC patients were divided into two groups: the *AIG1* up-regulated group and the *AIG1* down-regulated group. Kaplan–Meier curves showed significantly shorter survival times in patients in the *AIG1* down-regulated group than in the *AIG1* up-regulated group (Figure 4B).

4.4. AIG1 activates the NFAT signaling pathway in a dose-dependent manner

To investigate the potential role of AIG1 in cellular signaling pathways, a luciferase reporter system was employed, whereby an AIG1 expression plasmid was co-transfected with one of the following luciferase reporters: P21, HSE, NFAT, AP1, E2F, AP1 (PMA), Rb, NF-kappaB, p53, SRE, GRE or MYC. Interestingly, AIG1 was found to significantly enhance activity of the NFAT luciferase reporter by 1190% and the AP1 lucifercase reporter activity by 316%. In contrast, AIG1 reduced the activity of the p53 lucifercase reporter by 64.1% (*t*-test, $p < 0.03$, n = 4). No significant changes were observed in the activities of the P21, HSE, E2F, AP1 (PMA), Rb, NF-kappaB, SRE, GRE or MYC reporters (Figure 5A).

Since the NFAT signaling pathway was dramatically activated by the presence of AIG1, we next sought to check if this effect was dose-dependent. HEK293T cells were co-transfected with fixed amounts of pNFAT-Luc together with increasing amounts of pCMV-HA-AIG1 that were equalized by mock pCMV-HA. Quantification of reporter activity by luciferase assay determined that AIG1 did indeed induce activation of the

NFAT reporter in a dose-dependent manner (*t*-test, $p < 0.03$, n = 4) (Figure 5B).

5. DISCUSSION

Identifying the protein that interacts with a given protein is an important step toward understanding the functional responsibilities of that protein in the cell. We report here for the first time AIG1 interacts with Pirh2. After validating the interaction between Pirh2 and AIG1, we next sought to determine whether AIG1 could be ubiquitylated by Pirh2. However, there was no evidence that AIG1 and Pirh2 interact in this manner as determined by an *in vivo* ubiquitination assay (data not shown).

AIG1 belongs to the protein family containing FAR-17a domain. The first gene coding this domain was isolated from the hamster flank organ as one of the androgen-inducible genes (27). Up to now, the function of this kind of proteins is still unknown. Bioinformatics analysis shows that AIG1 could be a membrane protein. However, we found that AIG1 was restricted to cytoplasm around the nucleus in the Hela and HEK 293T cell lines by fluorescence microscopy analysis. This suggested that AIG1 at least partly localizes on nuclear membrane. Furthermore, RFP tagged AIG1 and GFP tagged Pirh2 can co-locate in the cytosol of HEK293T cells around the nucleus. This implied that the interaction between AIG1 and Pirh2 did not change the subcellular location of each other.

Although there is not significant correlation between the low expression level of *AIG1* and the differentiation of HCC, we found that the expression level of *AIG1* was positively related to the survival of HCC patients. Our results suggest that AIG1 might function as a tumor suppressor and could serve as a novel biomarker for the assessment of HCC prognosis. Notably, several other genes that are also specifically up- or down-regulated in HCCs, such as *DRH1* (10), *HDMCP* (12), *CD24* (28) and *MXR7* (29), have also been identified. Finally, we showed that NFAT signaling pathway can be activated by AIG1 with dose-dependent effect. In light of accumulating evidence pointing to a potential role of NFAT in the carcinogenesis and progression of HCCs (30-33), these results strongly suggest that AIG1 may be a novel factor/regulator in this process.

In summary, our studies suggest that AIG1 may be a novel candidate tumor suppressor, and the identification of its interaction with Pirh2 and its ability to activate the NFAT signaling pathway have provided important clues for future research on the role of AIG1 in tumor development.

6. ACKNOWLEDGMENT

Gang Wu and Meiqian Sun equally contributed to this work. We thank Dr. Yu Zhang for proofreading the manuscript and for critical discussions. This work was supported by the Chinese 863 program (Grant No. 2006AA02A310), CNHLPP program (Grant No. 2004BA711A19) and the Shanghai Science and Technology Developing Program (Grant No. 03DZ14024), which were awarded to K. Huo.

7. REFERENCES

1. D. M. Parkin, F. Bray, J. Ferlay and P. Pisani: Global cancer statistics, 2002. *CA Cancer J Clin*, 55(2), 74-108 (2005)

2. D. M. Parkin, F. Bray, J. Ferlay and P. Pisani: Estimating the world cancer burden: Globocan 2000. *Int J Cancer*, 94(2), 153-6 (2001)

3. P. Pisani, F. Bray and D. M. Parkin: Estimates of the world-wide prevalence of cancer for 25 sites in the adult population. *Int J Cancer*, 97(1), 72-81 (2002)

4. M. Sherman: Hepatocellular carcinoma: epidemiology, risk factors, and screening. *Semin Liver Dis*, 25(2), 143-54 (2005)

5. H. B. El-Serag: Hepatocellular carcinoma: recent trends in the United States. *Gastroenterology*, 127(5 Suppl 1), S27-34 (2004)

6. G. Fattovich, T. Stroffolini, I. Zagni and F. Donato: Hepatocellular carcinoma in cirrhosis: incidence and risk factors. *Gastroenterology*, 127(5 Suppl 1), S35-50 (2004)

7. M. A. Feitelson, B. Sun, N. L. Satiroglu Tufan, J. Liu, J. Pan and Z. Lian: Genetic mechanisms of hepatocarcinogenesis. *Oncogene*, 21(16), 2593-604 (2002)

8. B. Vogelstein and K. W. Kinzler: Cancer genes and the pathways they control. Nat Med, 10(8), 789-99 (2004)

9. Z. X. Wang, H. Y. Wang and M. C. Wu: Identification and characterization of a novel human hepatocellular carcinoma-associated gene. Br J Cancer, 85(8), 1162-7 (2001)

10. Y. Yamamoto, M. Sakamoto, G. Fujii, K. Kanetaka, M. Asaka and S. Hirohashi: Cloning and characterization of a novel gene, DRH1, down-regulated in advanced human hepatocellular carcinoma. Clin *Cancer Res*, 7(2), 297-303 (2001)

11. M. C. Moh, L. H. Lee, X. Yang and S. Shen: HEPN1, a novel gene that is frequently down-regulated in hepatocellular carcinoma, suppresses cell growth and induces apoptosis in HepG2 cells. *J Hepatol*, 39(4), 580-6 (2003)

12. M. G. Tan, L. L. Ooi, S. E. Aw and K. M. Hui: Cloning and identification of hepatocellular carcinoma down-regulated mitochondrial carrier protein, a novel liver-specific uncoupling protein. *J Biol Chem*, 279(43), 45235-44 (2004)

13. G. Z. Shao, R. L. Zhou, Q. Y. Zhang, Y. Zhang, J. J. Liu, J. A. Rui, X. Wei and D. X. Ye: Molecular cloning and characterization of LAPTM4B, a novel gene upregulated in hepatocellular carcinoma. *Oncogene*, 22(32), 5060-9 (2003)

14. L. K. Beitel, Y. A. Elhaji, R. Lumbroso, S. S. Wing, V. Panet-Raymond, B. Gottlieb, L. Pinsky and M. A. Trifiro: Cloning and characterization of an androgen receptor N-terminal-interacting protein with ubiquitin-protein ligase activity. *J Mol Endocrinol*, 29(1), 41-60 (2002)

15. R. P. Leng, Y. Lin, W. Ma, H. Wu, B. Lemmers, S. Chung, J. M. Parant, G. Lozano, R. Hakem and S. Benchimol: Pirh2, a p53-induced ubiquitin-protein ligase, promotes p53 degradation. *Cell*, 112(6), 779-91 (2003)

16. Zhang, L., J. Li, C. Wang, Y. Ma & K. Huo: A new human gene hNTKL-BP1 interacts with hPirh2. *Biochem Biophys Res Commun*, 330, 293-7 (2005)

17. Yan, J., D. Zhang, Y. Di, H. Shi, H. Rao & K. Huo: A newly identified Pirh2 substrate SCYL1-BP1 can bind to MDM2 and accelerate MDM2 self-ubiquitination. *FEBS Lett*, 584, 3275-8 (2010)

18. G. Wu, M. Sun, L. Zhang, J. Zhou, Y. Wang and K. Huo: A novel hPirh2 splicing variant without ubiquitin protein ligase activity interacts with p53 and is down-regulated in hepatocellular carcinoma. *FEBS Lett*, 584(13), 2772-8 (2010)

19. I. R. Logan, L. Gaughan, S. R. McCracken, V. Sapountzi, H. Y. Leung and C. N. Robson: Human PIRH2 enhances androgen receptor signaling through inhibition of histone deacetylase 1 and is overexpressed in prostate cancer. *Mol Cell Biol*, 26(17), 6502-10 (2006)

20. W. Duan, L. Gao, L. J. Druhan, W. G. Zhu, C. Morrison, G. A. Otterson and M. A. Villalona-Calero: Expression of Pirh2, a newly identified ubiquitin protein ligase, in lung cancer. *J Natl Cancer Inst*, 96(22), 1718-21 (2004)

21. M. Shimada, K. Kitagawa, Y. Dobashi, T. Isobe, T. Hattori, C. Uchida, K. Abe, Y. Kotake, T. Oda, H. Suzuki, K. Hashimoto and M. Kitagawa: High expression of Pirh2, an E3 ligase for p27, is associated with low expression of p27 and poor prognosis in head and neck cancers. *Cancer Sci*, 100(5), 866-72 (2009)

22. J. Seo, J. Kim and M. Kim: Cloning of androgen-inducible gene 1 (AIG1) from human dermal papilla cells. *Mol Cells*, 11(1), 35-40 (2001)

23. L. Li, Y. Shi, H. Wu, B. Wan, P. Li, L. Zhou, H. Shi and K. Huo: Hepatocellular carcinoma-associated gene 2 interacts with MAD2L2. *Mol Cell Biochem*, 304(1-2), 297-304 (2007)

24. K. J. Livak and T. D. Schmittgen: Analysis of relative gene expression data using real-time quantitative PCR and the 2(-Delta Delta C(T)) Method. *Methods*, 25(4), 402-8 (2001)

25. I. R. Logan, V. Sapountzi, L. Gaughan, D. E. Neal and C. N. Robson: Control of human PIRH2 protein stability: involvement of TIP60 and the proteosome. *J Biol Chem*, 279(12), 11696-704 (2004)

26. C. A. Corcoran, J. Montalbano, H. Sun, Q. He, Y. Huang and M. S. Sheikh: Identification and characterization of two novel isoforms of Pirh2 ubiquitin ligase that negatively regulate p53 independent of RING finger domains. *J Biol Chem*, 284(33), 21955-70 (2009)

27. T. Seki, R. Ideta, M. Shibuya and K. Adachi: Isolation and characterization of cDNA for an androgen-regulated mRNA in the flank organ of hamsters. *J Invest Dermatol*, 96(6), 926-31 (1991)

28. L. R. Huang and H. C. Hsu: Cloning and expression of CD24 gene in human hepatocellular carcinoma: a potential early tumor marker gene correlates with p53 mutation and tumor differentiation. *Cancer Res*, 55(20), 4717-21 (1995)

29. H. C. Hsu, W. Cheng and P. L. Lai: Cloning and expression of a developmentally regulated transcript MXR7 in hepatocellular carcinoma: biological significance and temporospatial distribution. *Cancer Res*, 57(22), 5179-84 (1997)

30. E. Lara-Pezzi, A. L. Armesilla, P. L. Majano, J. M. Redondo and M. Lopez-Cabrera: The hepatitis B virus X protein activates nuclear factor of activated T cells (NF-AT) by a cyclosporin A-sensitive pathway. *Embo J*, 17(23), 7066-77 (1998)

31. H. Lu, W. Ouyang and C. Huang: Inflammation, a key event in cancer development. *Mol Cancer Res*, 4(4), 221-33 (2006)

32. M. Mancini and A. Toker: NFAT proteins: emerging roles in cancer progression. *Nat Rev Cancer*, 9(11), 810-20 (2009)

33. A. Bergqvist, S. Sundstrom, L. Y. Dimberg, E. Gylfe and M. G. Masucci: The hepatitis C virus core protein modulates T cell responses by inducing spontaneous and altering T-cell receptor-triggered Ca2+ oscillations. *J Biol Chem*, 278(21), 18877-83 (2003)

Abbreviations: AIG1: androgen-induced 1; Pirh2: p53-induced RING-H2 protein; NFAT: nuclear factor of activated T cells; HCC: human hepatocellular carcinoma; ARNIP: androgen receptor N-terminal interacting protein; Mdm2: transformed mouse 3T3 cell double minute 2; AP1: activator protein 1; SRE: serum response element; GRE: glucocorticoid response element; HSE: heat shock response element; NF-kappaB: nuclear factor of kappa B cells; SPSS: SigmaStat statistical software package; GST: Glutathione S transferase; GFP: green fluorescent protein

Key Words: Pirh2, hepatocellular carcinoma, AIG1, NFAT signaling pathway, E3 ligase

Send correspondence to: Keke Huo, Institute of Genetics, School of Life Science, Fudan University, Shanghai 200433, PR China, Tel: 86-21-55664526, Fax: 86-21-55664526, E-mail: kkhuo@fudan.edu.cn

http://www.bioscience.org/current/vol3E.htm